Fifth International Conference on Sustainable Construction Materials and Technologies. http://www.claisse.info/Proceedings.htm

ELECTRICAL RESISTIVITY USED FOR LIQUID IMBIBITION MONITORING IN CEMENT-BASED MATERIALS: COMPARISON BETWEEN EXPERIENCE AND SIMULATION

Mohamed Abdou Ibro [a,1], Jérôme Verdier [a,2], Sandrine Geoffroy [a], Hugo Cagnon [a]

[a]Université de Toulouse, UPS, INSA, LMDC (Laboratoire Matériaux et Durabilité des Constructions),135 avenue de Rangueil, F-31077, Toulouse Cedex 4, France

[1]abdouibr@insa-toulouse.fr

[2] verdier@insa-toulouse.fr

ABSTRACT

Understanding capillary imbibition phenomena is of fundamental importance in many applications involving porous materials as water is the transport vector of aggressive agents. In this communication, an experimental and numerical study is carried out on capillary imbibition kinetics through two different concretes envisaged to be used for long term underground nuclear waste storage structures. The results of this experimental campaign show the influence of microstructure, height and initial degree of saturation on the sorptivity of the tested materials. The variability of the initial saturation of the materials shows that the presence of water in the porous network is a barrier to the imbibition phenomenon. The evolution of the water content profiles as well as the position of the liquid front over time is then evaluated using a non-destructive method based on electrical resistivity. A non-linear diffusion model commonly used to simulate drying is inverted to simulate capillary imbibition kinetics from sorption isotherms using a pore network model, which takes into account the hysteresis phenomenon. It has already been shown that the classical Washburn model for capillary rise adapted to homogeneous porous media shows long-term limitations in its applicability to cement-based materials. The theoretical approach proposed here shows very good agreements on the whole time range.

Keywords: Concrete, Capillary imbibition, Electrical resistivity, Modeling porous media

INTRODUCTION

Capillarity water absorption into civil engineering structure is a very important property that can be used to predict the durability, influenced mainly by moisture movements as well as chemical and biological agents it carries. There are many experimental studies of water imbibition through porous materials where the rate of water absorption is evaluated using gravimetric method [1]–[3]. This method allows accurate measurements of the total amount of water absorbed at a certain time but its distribution cannot be established. Thus, many authors have developed non-destructive (NDT) techniques that allow to observe how the degree of saturation varies spatially throughout the specimen by nuclear magnetic resonance [4], [5], neutron radiography [6]–[8], x-ray absorption [9], infrared thermography [10], [11], gamma rays [12]–[14], electrical resistivity [15]–[17]. Depending on the field of application, it is essential to know the limits of these techniques. Nuclear magnetic resonance is useful when observing materials like clay or sand, but for basic building materials like concrete or fired-clay brick, the signal is too weak [4]. This method allows testing of relatively small specimens only

[18]. Neutron radiography permits high-sensitive measurements of moisture concentration in porous materials in a broad range but, the experimental data obtained with this technique are significantly affected by experimental noise and by inhomogeneities in the porosity of the material under testing [18]. The main disadvantage of x-rays and infrared thermography is that they provide surface measurements, with very little penetrating radiation thus limiting investigation to specimens of small thickness [19]. With gamma rays method, limitations are imposed by several requirements: accessibility to both sides of the specimen, necessity for long exposure times, and safety precautions required to protect operators. The resistivity limit appears during evaluation at low saturation states which in reality are rarely reached in civil engineering structures. Indeed, the resistivity of concrete is strongly conditioned by continuity of its liquid phase. Hence, the particular interest that is given to this technique used in this study.

There are also numerical simulations, which attempt to explain the rate of water absorption. Capillary imbibition in a porous medium consisting of cylindrical tubes with constant cross-sections has been described quantitatively from Washburn [20] equation for a capillary tube. Dullien et al. [21] and Hammecker et al. [22], [2] by comparing the prediction of Washburn's model with experimental data showed that the model is not really appropriate for quantifying the capillary imbibition kinetics in the porous network of a sedimentary rock. Hall [1] and Gummerson et al. [4] have suggested that the absorption of water by porous building materials and the subsequent movement of water within these materials may be described by a nonlinear diffusion equation.

$$\frac{\partial \theta}{\partial t} = \frac{\partial}{\partial x}\left(D(\theta)\frac{\partial \theta}{\partial x}\right) \qquad (1)$$

Where θ is the volumetric water content [l/m^3] (volume of water per unit volume of porous medium), $D(\theta)$ is the hydraulic diffusivity [m^2/s], t is the time (s) and x is the spatial coordinate (m). Mainguy et al. [23] have developed a multiphase model considering gas pressure variations and based on the movements of the gas phase and liquid water. This non-linear diffusion model commonly used to simulate drying is inverted in this study to simulate capillary imbibition kinetics from sorption isotherms using a pore network model developed by Ranaivomanana et al. [24], [25] which is taking into account the hysteresis phenomenon.

Generally, imbibition tests are performed on dry specimens when in reality most of the structures are never completely dry or completely saturated, but they are mainly partially saturated. In addition, the most influential parameter governing transport properties is the moisture content and its distribution in the cement-based materials. It is therefore important to show how water absorption changes when there is a variability in the initial saturation of the material. In this paper, in addition to the gravimetric method, local evaluation of electrical resistivity has been applied to study moisture movement throughout the specimen. We also investigate the effects of the initial degree of saturation as well as the height of specimen on water absorption.

1 EXPERIMENTAL STUDY

1.1 Materials and Mixture Proportion

The experimental data used in this work were obtained by tests on two concretes; denoted C1 and C2, made respectively with Ordinary Portland Cement and Portland Slag Fly ash Cement, envisaged by the French National Agency for Radioactive Waste Management (ANDRA) for nuclear waste storage structures in deep geological formations. Table 1 summarized the mixture proportions and physical characteristics for each concrete. All materials were moist cured for a minimum of 28 days for C1 and 90 days for C2 before any testing. The specimens for moisture transport and electrical resistivity measurements were cylinders with a diameter of 11,2 cm. In order to highlight the influence of the specimen height, we tested 3 different heights (5, 10 and 20 cm). The porosity accessible to water is obtained according to the AFPC-AFREM protocol [26]. The degree of hydration is obtained from the formula proposed by Waller [27].

Table 1. Mixture proportions and physical characteristics for concrete C1 and C2

Material reference	C1	C2
Gravel content (kg/m^3) (5/12,5)	945	984
Sand content (kg/m^3) (0/4)	858	800
Cement content (kg/m^3)	400	450
Superplasticizer Masterglenium Sky 537 (kg/m^3)	3	4,5
Water-to-cement ratio (W/C)	0,43	0,39
Porosity accessible to water	0,132	0,139
Degree of hydration	0,758	0,724
Bulk density (kg/m^3)	2301	2281
Experimental water permeability (10^{-19} m^2)	0,95	1,4

1.2 Resistivity Measurements

1.2.1 Principle

In practice, electrical resistance R (Ohm) is directly measured by the testing device by using the direct application of Ohm's law (Fig. 1). Indeed, by applying a current I (A) between the two cross-sectional area of a specimen using plate electrodes (injection electrodes), a potential drop ΔV (V) is measured between these two electrodes. Resistivity ρ (Ohm.m) is an intrinsic characteristic of the material, and is independent of the geometry of the specimen. Equation (2) describes the relationship between the resistivity and resistance:

$$\rho = f.R = f.\frac{\Delta V}{I} \quad With\ f = \frac{A}{L} \qquad (2)$$

where R is the resistance of concrete; and f (m) is a geometrical factor which depends on the size and shape of the specimen as well as the distance between the electrodes on the testing device; A is the cross-sectional area (m^2) and L is the length of the specimen (m).

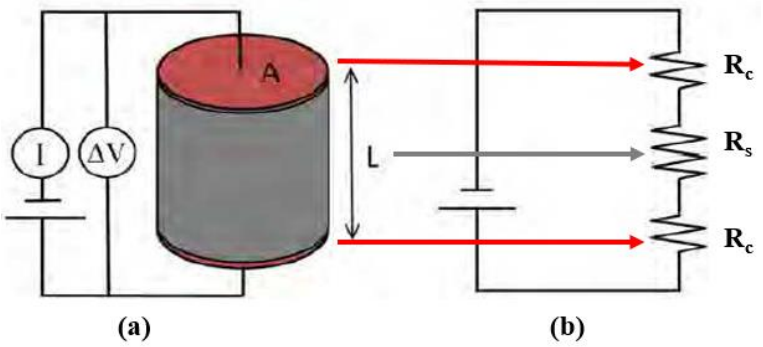

Fig. 1. 2-electrode resistivity measurement showing a diagram of the application of Ohm's law for specimens of uniform cross-section (a) and contact and specimen resistance (b) [17].

Fig. 1 shows an uncertainty on the resistance of the specimen (R_s) due to a contact resistance (R_c) that occurs at the electrode-specimen interface. R_c is a function of surface condition and moisture content of the specimen. Several approaches have been suggested to improve the contact between electrodes and concrete such as covering the surface area with wet sponges, conductive gels, electrolytic solutions or conductive paints [17].

1.2.2 Testing Procedure

In order to evaluate the overall resistivity of the specimens, two-point resistivity measurements are made on both sides of the cross-sections of the specimen. A device inspired by the multi-ring resistivity cell developed by Du plooy et al. [17] is set up to evaluate, in addition to the global resistivity, the local evolution of the resistivity. The new device consists of copper rings with a width of 0,3 cm uniformly spaced over the height of the sample at intervals of 2 cm, thus allowing the potential drop between any two electrodes to be measured (Fig. 2). A copper-based conductive paint applied to the ring-concrete interface reduces contact resistance (Rc) by ensuring very good and continuous electrode-concrete contact. In addition, this measuring device is interesting because it allows four-point Wenner measurement which is the most common way to determine the resistivity of concrete [28].

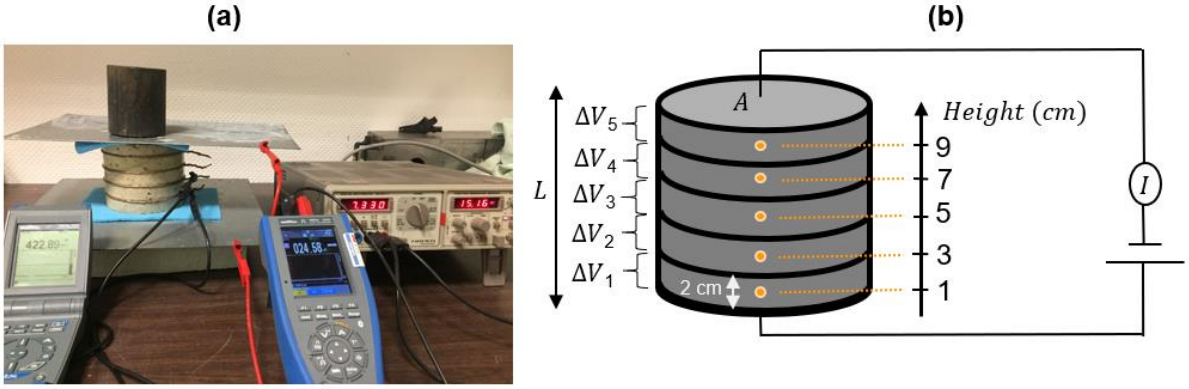

Fig. 2. Resistivity measuring device (a) and measuring principle (b) with copper rings

Wet sponges were used to ensure better contact between the concrete and the injection electrodes that are connected to a generator and the current used in the experimental campaign is an alternating current at a frequency of 15 Hz. The overall testing arrangement is displayed

in Fig. 2 (a) with a constant mass placed on the upper electrode to ensure uniform contact. The points represented in Fig. 2 (b) correspond to the position of the average resistivity calculated between two electrodes. For all configurations tested, the current is always imposed on plate electrodes larger than the cross-sectional area of the specimen. The modelling carried out on Comsol Multiphysics allows to obtain an uniform electrical field. The geometric analytical factor defined by Ohm's law (Eq. (1)) is therefore valid for our entire study.

1.3 Imbibition Test Procedure

Imbibition tests are performed on specimen with variable initial degree of saturation. The specimens were dried at 50°C to reach global saturation states of 0,6 and 0,3 and then at 80°C to reach the dry state (approximatively global saturation state of 0,03 considering that the total free water is removed for drying at 105°C). The preconditioning is finalized with a moisture redistribution phase. The specimens are wrapped in cellophane paper and then sealed with self-adhesive aluminium foil and returned to the same drying temperature for a time equal to the drying time. The specimens, which have been preconditioned to the various saturation states, are then instrumented with copper rings to ensure resistivity measurements over the entire height of the specimens. The lateral surface of the specimens is then waterproofing with resin. Then, the bottom flat face of the specimens is put into contact with water, only two millimetres below the water level which is kept constant throughout the test period by an overflow system (Fig. 3). The sample gains weight due to water rise, registered at regular time intervals to evaluate the rate of water absorption. Water absorption measurement is generally performed over a few hours. But it is necessary to study capillary imbibition over a longer period of time for materials used for long-term storage. So, in this study the test is carried out until the mass stabilizes, which may go beyond one month for some specimens.

Fig. 3. Experimental device for the capillary imbibition test

2 MODELLING OF WATER ABSORPTION IN POROUS MEDIA

Mainguy et al. [23], [29], [30] have developed a multiphase model where moisture transfers are described by the movements of the gas phase and liquid water. In this model, the solid skeleton is considered to be non-deformable, the liquid phase incompressible, the water transfers are isothermal at 20° C and the forces of gravity negligible. This hypothesis of neglecting gravity is not harmful as Hall and Hoff [31] have shown on walls of great heights (50 to 100 cm) that capillary forces are dominant and the effects of gravity can be neglected. The gas phase consists

of a mixture of two perfect gases, dry partial pressure air P_a and water vapour partial pressure P_v. The total pressure P_g of the mixture is assumed to be ideal:

$$P_g = P_a + P_v \quad (3)$$

This model is based on macroscopic mass conservation equations of each components present in the porous media:

$$\begin{cases} \dfrac{\partial(\emptyset S_w \rho_w)}{\partial t} = -div\left[-\rho_w \dfrac{K_w}{\mu_w} k_{rw} \overrightarrow{grad} P_w\right] - \dot{\mu} \\ \dfrac{\partial[\emptyset \rho_v (1-S_w)]}{\partial t} = -div\left[-\dfrac{P_v M_v K_g}{RT\mu_g}\left(k_{rg} + \dfrac{\beta}{P_g}\right)\overrightarrow{grad} P_g - \dfrac{P_g M_v}{RT} D \overrightarrow{grad}\left(\dfrac{P_v}{P_g}\right)\right] + \dot{\mu} \\ \dfrac{\partial[\emptyset \rho_a (1-S_w)]}{\partial t} = -div\left[-\dfrac{P_a M_a K_g}{RT\mu_g}\left(k_{rg} + \dfrac{\beta}{P_g}\right)\overrightarrow{grad} P_g - \dfrac{P_g M_a}{RT} D \overrightarrow{grad}\left(\dfrac{P_a}{P_g}\right)\right] \end{cases} \quad (4)$$

ρ_i refers to the density of component i (w, v or a respectively for liquid water, vapor and dry air). $\emptyset$ and S_w refer respectively to porosity accessible to water and liquid water saturation rate. The quantities $(\emptyset S_w \rho_w)$; $[\emptyset \rho_v (1-S_w)]$; $[\emptyset \rho_a (1-S_w)]$ in the terms of time derivation correspond respectively to the masses of water vapor, liquid water and dry air contained in a unit volume of material. Divergence operators for mass flows correspond to mass exchanges with the outside. K_i is the intrinsic permeability of fluid i (m^2); k_{ri} is the relative permeability of fluid i (-); R is the perfect gas constant (8.32 J/mol/kg); T is the temperature (K); M_i is the molecular weight of fluid *i* (kg/mol); D is the diffusion coefficient of the gaseous components (m^2/s) involving water vapor diffusion reduction factor R_d(-); β represents the slippery part of the movement of the gas phase (P_a). Finally, $\dot{\mu}$ refers to phase changes, the mass of water that passes from the liquid phase to the gas phase. For the modeling, besides accessible porosity $\emptyset$ obtained experimentally, the other input data identified above are evaluated from the porous network model developed by Ranaivomanana et al.[24], [25]. Since this model allows the hysteresis to be taken into account, the adsorption isotherms from the different initial global saturation degree (S_{wi}) are considered in the modelling. In Table 2 below, we give the values of intrinsic permeability to water (K_w) allowing the best experimental kinetics to be restored as well as the experimental height reached by the wetting front (h_w) allowing the bearing to be found at the end of the imbibition test of each materials considered for the modelling.

Table 2. Calibration parameters of each of the materials considered for modelling

Material reference	C1 5 cm			C1 10cm	C1 20cm	C2 5 cm			C2 10cm	C2 20cm
S_{wi}	0	0,3	0,6	0,6	0,6	0	0,3	0,6	0,6	0,6
K_w (10^{-19} m^2)	5	5	1	2	1	4	1,8	1	1,8	1,8
h_w (cm)	5	4,8	4	4,7	6,3	5	4,8	2,25	3,2	3,5

3 RESULTS AND COMMENTS

Results presented in Fig. 4 and

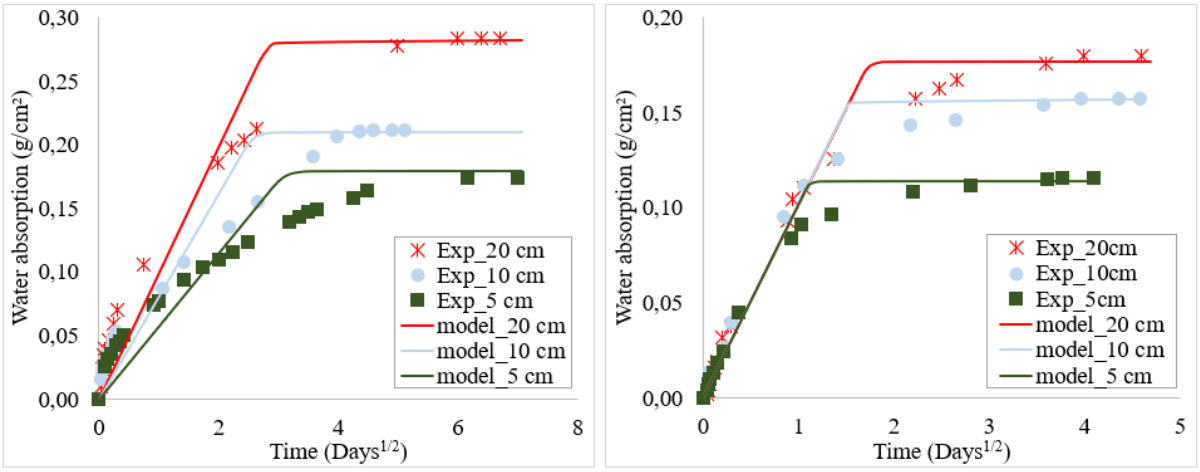

Fig. **5** show the mass variation of the absorbed water per unit cross section plotted as a function of the square root of imbibition time for all studied materials. A deviation from the theoretical expectation of a linear relationship with the square root of time in the cumulative absorption curve is observed in both short and long term especially for materials with a high initial saturation state. This anomaly consisting of a considerable slowdown in the absorption rate compared to its initial value has already been observed by many researchers [7], [32]. They explain this phenomenon by a new hydration, which takes place in the presence of water and causes an increase of effective grain size and tends to block the micropores. In our case, this phenomenon is considered low due to the curing periods respected and the advanced hydration of the materials. The obstruction to the movement of water through the porous structure can be attributed to the presence of a water profile in the porous network. This constitutes a barrier to the imbibition phenomenon. In fact, if at the end of the re-distribution, the profile is not constant, the border is below the desired saturation level, resulting in a faster imbibition kinetics at the beginning. Then, on the part above the desired saturation level, the imbibition kinetics is slower. For a given initial water saturation, the slight differences in water absorption kinetics observed between C1_5 cm (a) and C2_5 cm (b) can be explained by a difference in microstructure (due to pozzolanic additions) despite similar water porosities.

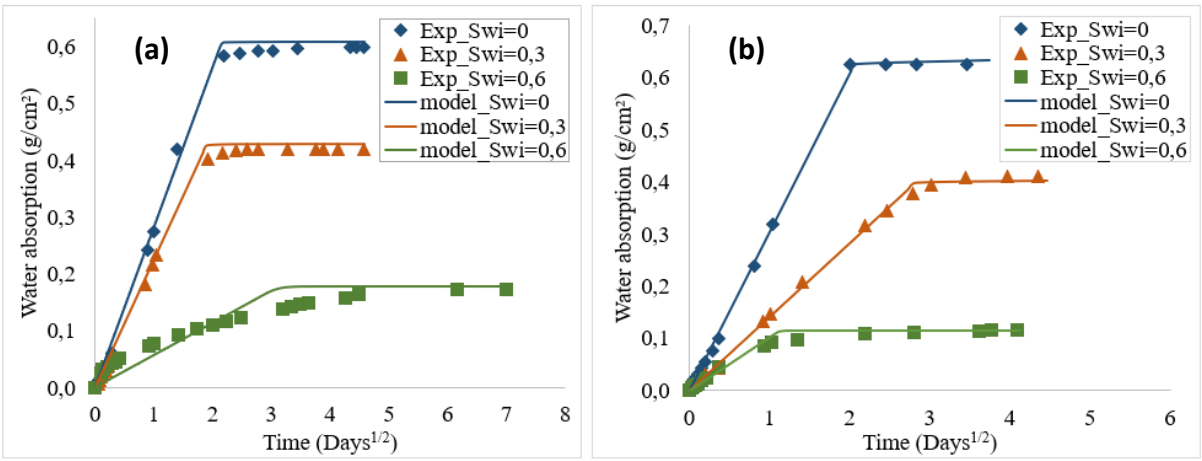

Fig. 4. Comparison between theoretical and experimental results of capillary absorption

for C1_5 cm (a) and C2_5 cm (b)

Let's turn to the analysis of the influence of height on water absorption. For a given initial water saturation (S_{wi}=0,6),

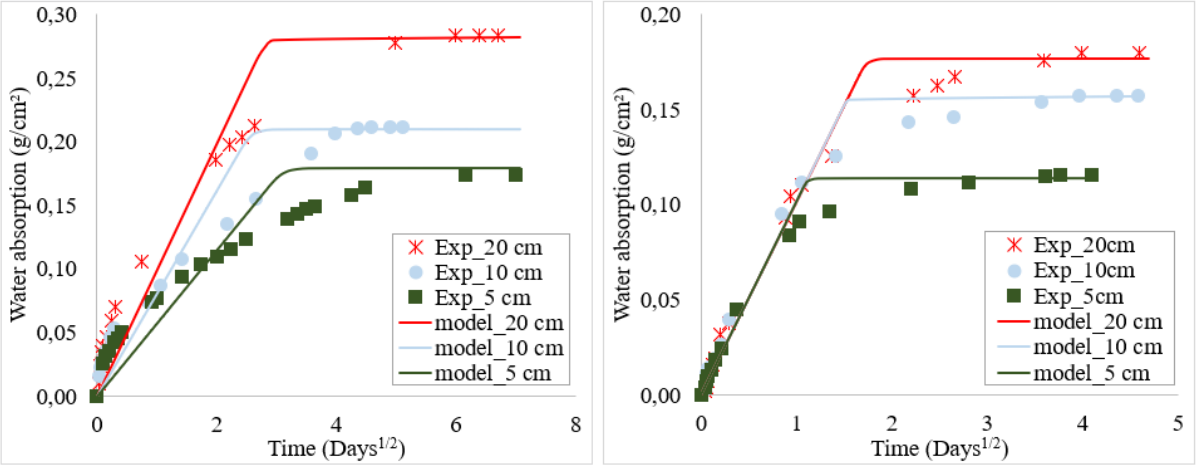

Fig. **5** shows significant differences in kinetics. The water absorption increases as material height increases. Similarly, the gap identified between C1_S_{wi}=0,6 (a) and C2_ S_{wi}=0,6 (b) becomes larger as the height rise. Assuming that re-distribution is more effective on specimen of lower height, it appears that water advance front encounters more resistance on materials of higher height (Table 2). Some researchers (Liu [33]; Hall and Hoff [34]) attribute the dependence of size and shape on the water absorption height to the resistance of the pressure of the air in the pores of concrete matrix that water has to overcome. The pressure can be higher or lower depending on size and moisture distribution of the tested specimen.

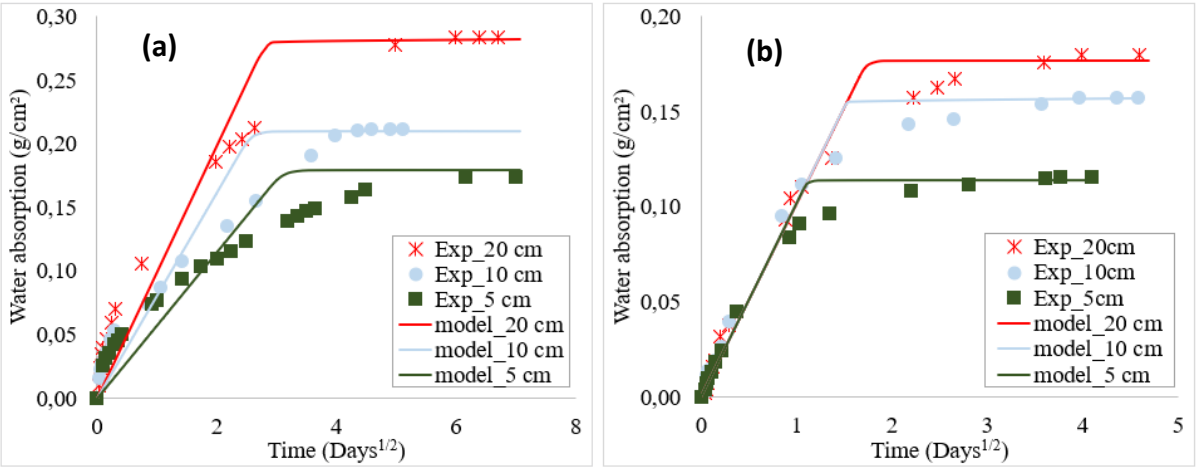

Fig. 5. Comparison between theoretical and experimental results of capillary absorption

for C1_Swi=0,6 (a) and C2_ Swi=0,6 (b)

The differences in evolution as a function of initial saturation and height observed in Fig. 4 and

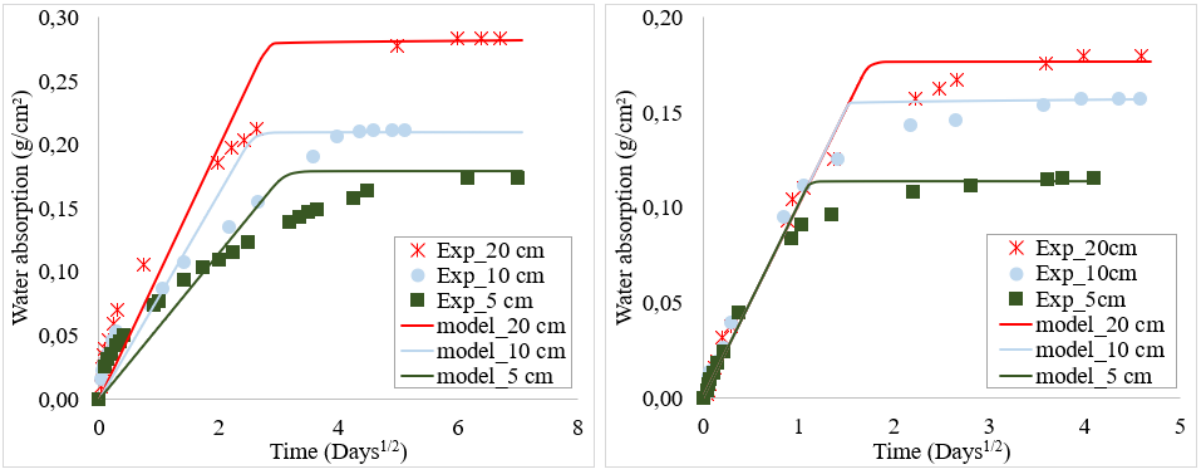

Fig. **5** can also be attributed to the development of microcracks within the porous structure. Indeed, even if the preconditioning is done to dry the specimens at temperatures lower than the one usually used (105°C), Wong et al. [35] have shown that micro-cracking occurs with drying from 50 °C due to shrinkage and strength heterogeneities between cement paste and granular phases. As a material is dried to reach lower saturation states, new cracks appear that could create new access paths to pores that were not accessible. This could partly explain the increase in intrinsic permeability K_w with drying observed in Table 2. The intrinsic permeability values considered for the modeling (Table 2) correspond with the same range of quantities to the experimental values in Table 1. In Fig. 4 and

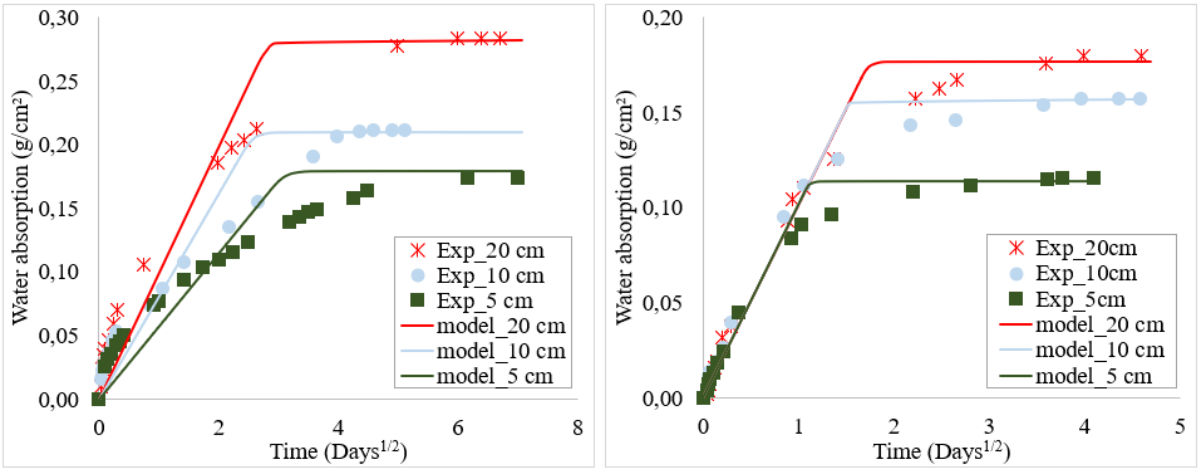

Fig. **5** the model allows to correctly predict capillary imbibition kinetics on the least initially saturated materials (S_{wi}=0 and 0,3). However, a poorer correlation with the most initially saturated materials (S_{wi}=0,6) is observed. This can be explained by the fact that the water profiles mentioned earlier are less marked on the initially less saturated materials. As all materials have been subjected to a moisture redistribution phase at the end of preconditioning, the modelling was carried out initially considering a constant water saturation profile in the material. Nevertheless, noting the non-linearity of the experimental evolutions, the hypothesis of a constant profile can be questioned. Thus, taking into account a real initial profile could make it possible to correct the model predictions by increasing the water rise at the beginning and reducing it at the core. This approach is not presented in this paper.

The evolution of resistivity as a function of height during the imbibition test is represented in Fig. 6. As mentioned above, the points represented correspond to the average resistivity calculated between two electrodes. It should be noted that in reality, between two electrodes, the most saturated part of the specimen should have a lower resistivity. Despite the preconditioning with a moisture redistribution phase, a non-constant resistivity profile is observed before starting the imbibition test (t=0). The preconditioning consisting in redistributing the moisture during a time corresponding to the drying time does not allow to reach a constant profile in the material. The decrease in resistivity values during the imbibition time reveals the evolution of the water front in the concrete until it stabilizes. This decrease in resistivity is observed up to the height corresponding to the experimental height reached by the wetting front. The decrease in resistivity observed on the upper surface of the sample is an artifact due to the use of a wet sponge at the testing moment. The lack of knowledge of the contact resistance leads to incertitude on the measuring rings closest to the injection electrode. An overestimation of the average resistivities at 1 cm and 9 cm height is observed over the entire test period.

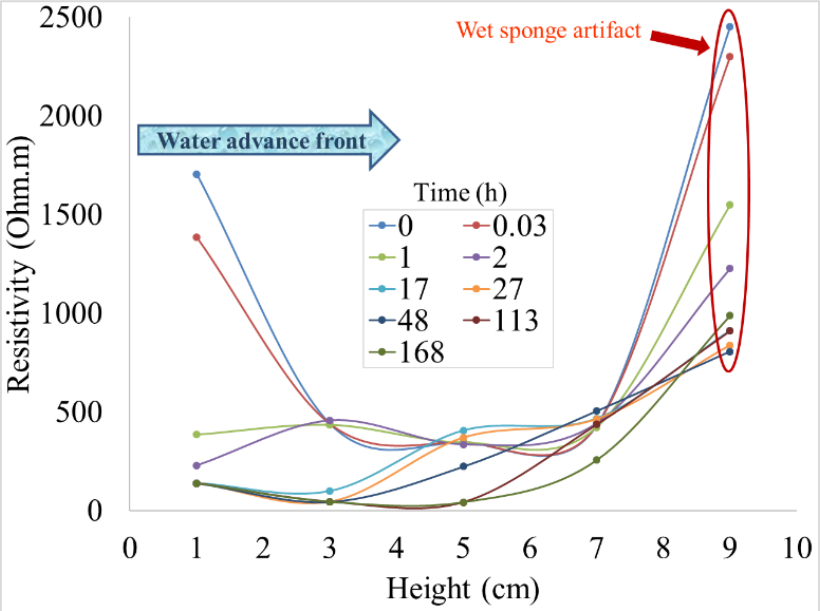

Fig. 6. Local monitoring during the imbibition test of resistivities on concrete C1_10cm (S_{wi}= 0,6)

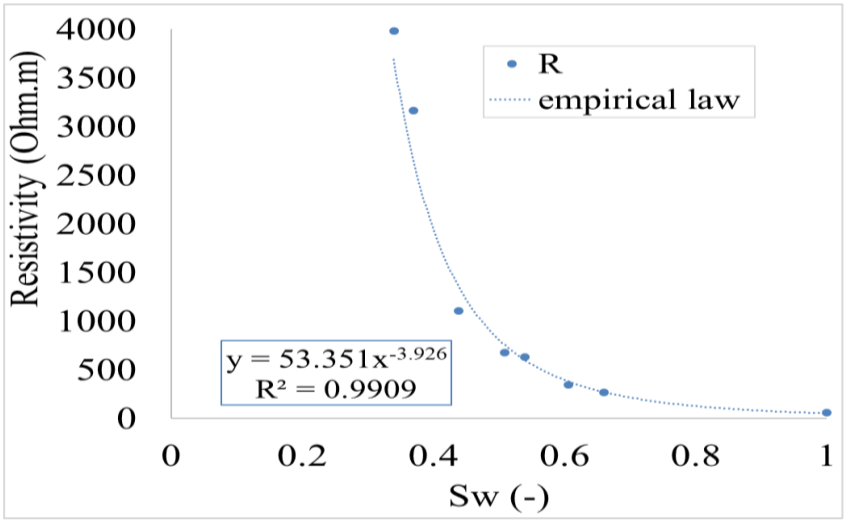

Fig. 7. Empirical law of resistivity as a function of water saturation (a) in order to find the saturation profiles for C1_10cm (Swi= 0,6) (b)

A non-linear relationship trend is observed between moisture content and electrical resistivity values obtained experimentally (Fig. 7). This same evolution has been highlighted in many studies [15]–[17]. The pozzolanic additions present in C2 give it a finer pore distribution. Bijen [36] has shown that this densification of the cementitious matrix reduces diffusivity of ions. This reduction is thus reflected in other related properties, such as electrical resistivity which increases with the presence of pozzolanic additions. Using the empirical law on the resistivity profiles of concrete C1_10cm (S_{wi}= 0,6), the saturation profiles are thus deduced in Fig. 8 (a). The evolution of local saturation within the material is shown to increase during the imbibition time for both the experimental evaluation (Fig. 8(a)) and the model (Fig. 8 (b)). The comparison of experimental and numerical saturation evolutions shows similarities in particular with regard to the depth reached by the water advance front over time. Indeed, at 17 hours, the experimental water advance front begins to reach a depth of 2 cm, which corresponds to the model's prediction. Then in the longer term it appears that the experimental front advances faster than the model with a reasonable gap. For example, at 27 and 48 hours, the experimental front is respectively between 1 to 3 cm and then between 3 to 5 cm while the model reaches a depth of 2 cm at 27 hours then approximately 3 cm at 48 hours.

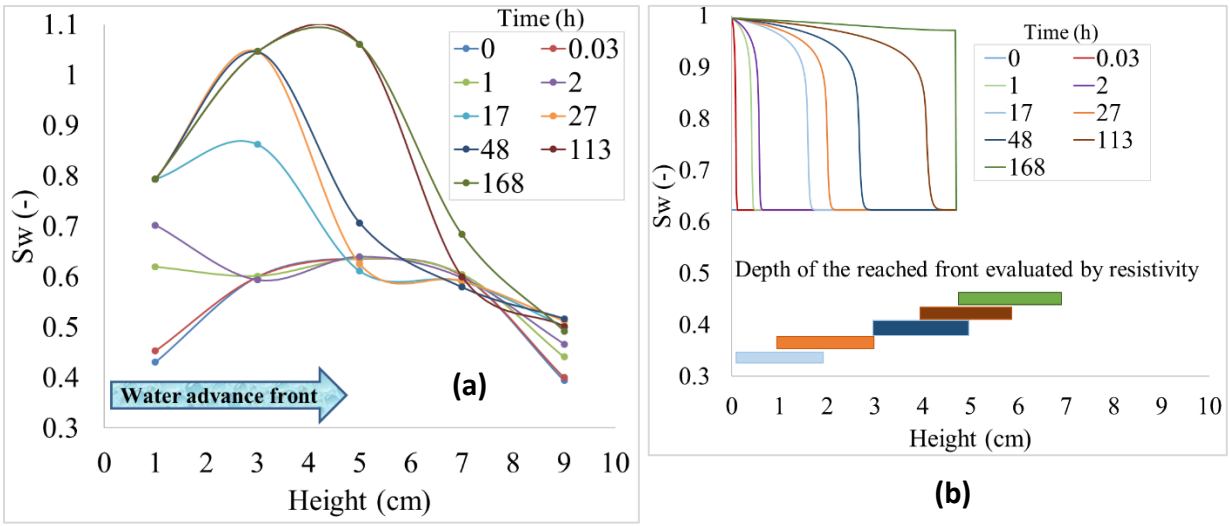

Fig. 8. Saturation profile found from the experimental resistivities (a) and model (b)

CONCLUSIONS

In this paper, the influence of the initial water saturation as well as the height of the materials tested on capillary water rise during absorption tests has been demonstrated. To do this, a new experimental protocol different from the usual procedure used for imbibition tests, in particular with regard to preconditioning and imbibition time has been adopted. The analysis of the evolution obtained on different materials leads to the conclusion that water absorption by capillarity is strongly related to the microstructure, the height of the materials tested and particularly to the degree of initial saturation of the material. The results of the evolutions at initial saturation degree of 0,3 and dry state for 10 cm and 20 cm high specimens are not yet available. Nevertheless, it can be observed from the results presented that the rate of water absorption falls with increasing initial water saturation and rise with increasing the height of the materials.

This paper established quantitative relationship of resistivity with local water saturation. Relationship between water saturation and resistivity values obtained experimentally, demonstrates a non-linear correlation. A methodology has been presented to study water distribution profile within cement-based materials using electrical resistivity. This technique delivered quantitative data giving local water contents evolution using a non-linear empirical law of resistivity as a function of water saturation.

The water absorption rates by low-rise materials with varying degrees of water saturation are in good agreement with the non-linear diffusion model developed by Mainguy et al. [23]. However, improvements are to be expected in order to take into account an imbibition resistance factor into the model for materials that are initially highly saturated or of high height. It was highlighted that a first approach without modifying the physics of the model would be to take into account a non-constant saturation profile within the tested materials. Then, it will be necessary to account for this resistance factor by integrating into the physics of the model a

consideration of some phenomena such as micro-cracking as well as the non-dissipated part of the gaseous overpressures within the tested materials.

REFERENCES

[1] C. Hall, « Water sorptivity of mortars and concretes: a review », *Mag. Concr. Res.*, vol. 41, n° 147, p. 51-61, juin 1989.

[2] C. Hammecker et D. Jeannette, « Modelling the capillary imbibition kinetics in sedimentary rocks: Role of petrographical features », *Transp. Porous Media*, vol. 17, n° 3, p. 285–303, 1994.

[3] W. J. McCarter, H. Ezirim, et M. Emerson, « Properties of concrete in the cover zone: water penetration, sorptivity and ionic ingress », *Mag. Concr. Res.*, vol. 48, n° 176, p. 149-156, sept. 1996.

[4] R. J. Gummerson, C. Hall, W. D. Hoff, R. Hawkes, G. N. Holland, et W. S. Moore, « Unsaturated water flow within porous materials observed by NMR imaging », *Nature*, vol. 281, n° 5726, p. 56, 1979.

[5] A. Leventis, D. A. Verganelakis, M. R. Halse, J. B. Webber, et J. H. Strange, « Capillary Imbibition and Pore Characterisation in Cement Pastes », *Transp. Porous Media*, vol. 39, n° 2, p. 143-157, mai 2000.

[6] H. Justnes, K. Bryhn-Ingebrigtsen, et G. O. Rosvold, « Neutron radiography: an excellent method of measuring water penetration and moisture distribution in cementitious materials », *Adv. Cem. Res.*, vol. 6, n° 22, p. 67–72, 1994.

[7] L. Hanžič et R. Ilić, « Relationship between liquid sorptivity and capillarity in concrete », *Cem. Concr. Res.*, vol. 33, n° 9, p. 1385–1388, 2003.

[8] A. Shafizadeh *et al.*, « Quantification of water content across a cement-clay interface using high resolution neutron radiography », *Phys. Procedia*, vol. 69, p. 516–523, 2015.

[9] G. Sant et J. Weiss, « Using X-ray absorption to assess moisture movement in cement-based materials », *J. ASTM Int.*, vol. 6, n° 9, p. 1–15, 2009.

[10] E. Barreira, R. M. S. F. Almeida, et J. M. P. Q. Delgado, « Infrared thermography for assessing moisture related phenomena in building components », *Constr. Build. Mater.*, vol. 110, p. 251-269, mai 2016.

[11] M. Bianchi Janetti, L. P. M. Colombo, F. Ochs, et W. Feist, « Determination of the water retention curve from drying experiments using infrared thermography: A preliminary study », *Int. J. Therm. Sci.*, vol. 114, p. 271-280, avr. 2017.

[12] M. K. Kumaran et M. Bomberg, *A gamma-spectrometer for determination of density distribution and moisture distribution in building materials*. National Research Council Canada. Division of Building Research, 1985.

[13] J. Cid, J. F. Alquier, et P. Crausse, « Study of moisture transfer in a deformable porous medium through attenuation of two different energy gamma rays », *Rev. Sci. Instrum.*, vol. 63, n° 3, p. 2057–2064, 1992.

[14] G. Villain et M. Thiery, « Gammadensimetry: A method to determine drying and carbonation profiles in concrete », *Ndt E Int.*, vol. 39, n° 4, p. 328–337, 2006.

[15] M. Saleem, M. Shameem, S. E. Hussain, et M. Maslehuddin, « Effect of moisture, chloride and sulphate contamination on the electrical resistivity of Portland cement concrete », *Constr. Build. Mater.*, vol. 10, n° 3, p. 209-214, avr. 1996.

[16] J.-K. Su, C.-C. Yang, W.-B. Wu, et R. Huang, « Effect of moisture content on concrete resistivity measurement », *J. Chin. Inst. Eng.*, vol. 25, n° 1, p. 117-122, janv. 2002.

[17] R. Du Plooy, S. P. Lopes, G. Villain, et X. Derobert, « Development of a multi-ring resistivity cell and multi-electrode resistivity probe for investigation of cover concrete condition », *NDT E Int.*, vol. 54, p. 27–36, 2013.
[18] M. I. Nizovtsev, S. V. Stankus, A. N. Sterlyagov, V. I. Terekhov, et R. A. Khairulin, « Determination of moisture diffusivity in porous materials using gamma-method », *Int. J. Heat Mass Transf.*, vol. 51, nº 17, p. 4161-4167, août 2008.
[19] P. Priyada et R. Ramar, « Determining the water content in concrete by gamma scattering method », *Ann. Nucl. Energy*, vol. 63, p. 565–570, 2014.
[20] E. W. Washburn, « The dynamics of capillary flow », *Phys. Rev.*, vol. 17, nº 3, p. 273, 1921.
[21] F. A. L. Dullien, M. S. El-Sayed, et V. K. Batra, « Rate of capillary rise in porous media with nonuniform pores », *J. Colloid Interface Sci.*, vol. 60, nº 3, p. 497–506, 1977.
[22] C. Hammecker, J.-D. Mertz, C. Fischer, et D. Jeannette, « A geometrical model for numerical simulation of capillary imbibition in sedimentary rocks », *Transp. Porous Media*, vol. 12, nº 2, p. 125–141, 1993.
[23] M. Mainguy, O. Coussy, et V. Baroghel-Bouny, « Role of air pressure in drying of weakly permeable materials », *J. Eng. Mech.*, vol. 127, nº 6, p. 582–592, 2001.
[24] H. Ranaivomanana, J. Verdier, A. Sellier, et X. Bourbon, « Toward a better comprehension and modeling of hysteresis cycles in the water sorption–desorption process for cement based materials », *Cem. Concr. Res.*, vol. 41, nº 8, p. 817–827, 2011.
[25] H. Ranaivomanana, J. Verdier, A. Sellier, et X. Bourbon, « Prediction of relative permeabilities and water vapor diffusion reduction factor for cement-based materials », *Cem. Concr. Res.*, vol. 48, p. 53–63, 2013.
[26] A. AFREM, « Méthodes recommandées pour la mesure des grandeurs associées à la durabilité », *C. r. Journ. Tech. AFPC-AFREM Durabilité Bétons*, 1997.
[27] V. Waller, « Relations entre composition des bétons, exothermie en cours de prise et résistance en compression », PhD Thesis, Ecole des Ponts, 1999.
[28] K. Gowers et S. Millard, « Measurement of concrete resistivity for assessment of corrosion », *ACI Mater. J.*, vol. 96, nº 5, 1999.
[29] M. Mainguy, O. Coussy, et R. Eymard, « Modelisation des transferts hydriques isothermes en milieu poreux. Application au sechage des materiaux a base de ciment », *ETUDES Rech. Lab. PONTS CHAUSSEES - Ser. OUVRAGES ART*, nº OA 32, juill. 1999.
[30] O. Coussy, « Mecanique des milieux poreux (Editions Technip, Paris, 1991) », *Google Sch.*
[31] C. Hall et W. D. Hoff, « Rising damp: capillary rise dynamics in walls », *Proc. R. Soc. Math. Phys. Eng. Sci.*, vol. 463, nº 2084, p. 1871–1884, 2007.
[32] C. Hall *et al.*, « Water anomaly in capillary liquid absorption by cement-based materials », *J. Mater. Sci. Lett.*, vol. 14, nº 17, p. 1178–1181, 1995.
[33] Z. Liu, « Frost Deterioration in Concrete Due to Deicing Salt Exposure: Mechanism, Mitigation and Conceptual Surface Scaling Model. », 2014.
[34] C. Hall et W. D. Hoff, *Water transport in brick, stone and concrete*. CRC Press, 2009.
[35] H. S. Wong, M. Zobel, N. R. Buenfeld, et R. W. Zimmerman, « Influence of the interfacial transition zone and microcracking on the diffusivity, permeability and sorptivity of cement-based materials after drying », *Mag Concr Res*, vol. 61, nº 8, p. 571–589, 2009.
[36] J. Bijen, « Benefits of slag and fly ash », *Constr. Build. Mater.*, vol. 10, nº 5, p. 309–314, 1996.